Polymer 51 (2010) 5369–5376

Contents lists available at ScienceDirect

Polymer

journal homepage: www.elsevier.com/locate/polymer

Studies on syntheses and morphology characteristic of chiral novel poly(ester-imide)/TiO_2 bionanocomposites derived from L-phenylalanine based diacid

Shadpour Mallakpour [a,b,*], Samaneh Soltanian [a]

[a] Organic Polymer Chemistry Research Laboratory, Department of Chemistry, Isfahan University of Technology, Isfahan 84156-83111, Islamic Republic of Iran
[b] Nanotechnology and Advanced Materials Institute, Isfahan University of Technology, Isfahan 84156-83111, Islamic Republic of Iran

ARTICLE INFO

Article history:
Received 8 July 2010
Received in revised form
21 September 2010
Accepted 25 September 2010
Available online 1 October 2010

Keywords:
Optically active polymer
Bionanocomposites
Poly(ester-imide)

ABSTRACT

In this study, a new optically active poly(ester-imide) (PEI) was synthesized from the polymerization reaction of N,N′-(pyromellitoyl)-bis-L-phenylalanine diacid with 4,4′-thiobis(2-tert-butyl-5-methylphenol) using tosyl chloride, pyridine and N,N-dimethyl formamide as a condensing agent. The obtained polymer and inorganic metal oxide bionanocomposites composed of poly(ester-imide)/titanium dioxide were synthesized through ultrasonic irradiation. The formation of PEI was confirmed by ^{1}H NMR, fourier transform IR spectroscopy (FT-IR), specific rotation and elemental analysis. The resulting bionanocomposites were characterized by FT-IR, powder X-ray diffraction (XRD), atomic force microscopy)AFM(, scanning electron microscopy (SEM), field emission scanning electron microscopy (FE-SEM), transmission electron microscopy (TEM) and thermogravimetric analysis (TGA). The TEM, SEM and FE-SEM results indicated that the nanoparticles were dispersed homogeneously in PEI matrix on nanoscale. TGA confirmed that the heat stability of the nanocomposite was improved in the presence of TiO_2 nanoparticles.

1. Introduction

Composite materials containing polymeric and inorganic units have been attracting considerable attention as new materials because they have novel optical, [1–3] mechanical, [4] electronic properties, [5] as well as cosmetic and medicine applications [6]. The applications of inorganic particles and analogous hybrid polymer-inorganic composite material became imperative when chemists, material scientists and physicists recognized that reduction in dimensions of the particles results in the manifestation of a new crystal motif, or conceivably a new physical phenomenon that does not exist in materials with larger particle sizes [7].

Nanocomposites including biocompatible polymer matrix and inorganic nanoparticle filler symbolize a novel group of composite biomaterials for tissue engineering, scaffolds and biomedical implants and devices. Titanium dioxide (TiO_2) is one of the most studied metal oxides in recent years, since it is economical and nontoxic material, which has high refractive index and possesses the ability to absorb ultraviolet light. TiO_2 can act as a bioactive ceramic in the sense that some shapes of TiO_2 show a strong interfacial bonding to alive tissue by way of the creation of a biologically active hydroxyapatite layer on the material surface [8,9]. TiO_2 nanoparticles crystallize into three polymorphic forms: rutile, anatase and brookite. The rutile shape is stable at high temperatures and is generally obtained when pure TiO_2 crystal is produced. Anatase structure is less stable and forms at lower temperatures and is chemically and optically more active in environmental remediation than rutile particles. Brookite form occurs only in excessive conditions and is very rare. The anatase to rutile transition is an irreversible procedure and usually happens within a temperature range of 500–1000 °C [10]. Because of photocatalytic effects of TiO_2 nanoparticles, they could decay a variety of organic chemicals such as aldehyde, toluene and polymers for instance polyethylene [11,12], polypropylene [13], polyvinylchloride [14] and polystyrene [15]. Addition of TiO_2 in macromolecule matrix can supply substantial enhancement in the weatherability and durability of polymer products [8].

Ultrasonic irradiation has been broadly used in chemistry, medicine, cleaning, machining, jointing and preparing nanocomposites [16–20]. This rout can control the size distribution and morphology of the nanosized particles. As was known, the aggregation of nanoparticles is decreased and its dispersivity is highly improved [21].

Poly(ester-imide)s (PEI)s contain both ester and heterocycle imide structures along the main chain of the polymer backbone and

* Corresponding author. Nanotechnology and Advanced Materials Institute, Isfahan University of Technology, Isfahan 84156-83111, Islamic Republic of Iran. Tel.: +98 311 391 3267; fax: +98 311 391 2350.
E-mail addresses: mallak@cc.iut.ac.ir, mallak777@yahoo.com, mallakpour84@alumni.ufl.edu (S. Mallakpour).

0032-3861/$ – see front matter © 2010 Elsevier Ltd. All rights reserved.
doi:10.1016/j.polymer.2010.09.063

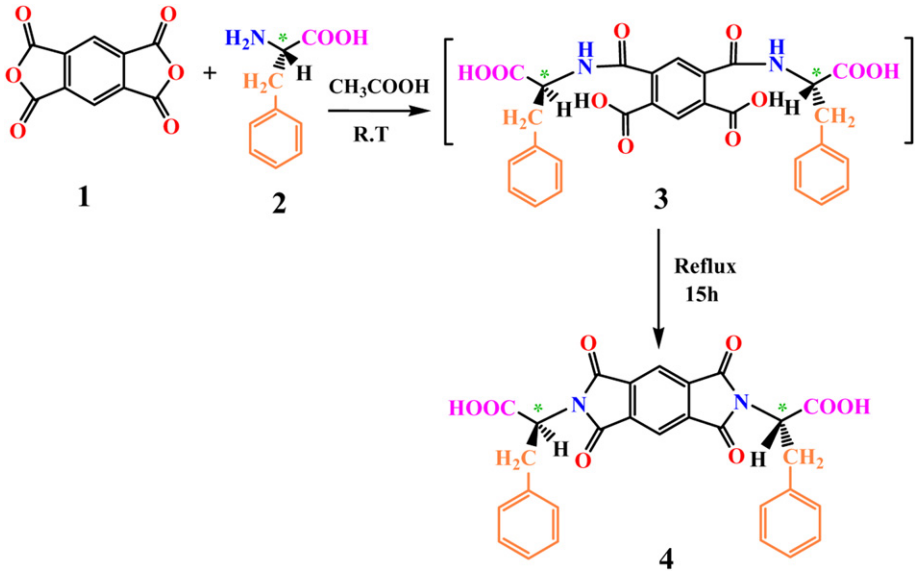

Scheme 1. Synthesis of diacid (4).

possess high thermal stabilities, and are used as high-strength and high-modulus fibers, as well as high-performance engineering resins [22], being a promising matrix candidate for hybrid materials. Chiral polymers have attracted a large deal of interest in the applications of fields for instance drug delivery, tissue engineering, dentistry and chiral stationary phases for resolution of enantiomers in chromatographic techniques [23–25] due to their promising properties.

In this work, a novel optically active PEI having good thermal stability as well as good solubility in common organic solvent, was prepared, by direct polycondensation of optically active natural amino acid based diacid and an aromatic diol using Vilsmeier adduct derived from tosyl chloride (TsCl) and N,N-dimethylformamide (DMF) in pyridine (Py) as a condensing agent. Then optically active poly(ester-imide)/titanium dioxide (PEI/TiO_2) bionanocomposites were synthesized under ultrasonic irradiation. The resulting bionanocomposites are characterized by various techniques including FT-IR, XRD, TGA and their morphology were investigated by SEM, FE-SEM, AFM and TEM analyses.

2. Experimental

2.1. Materials

All chemicals were purchased from Fluka Chemical Co. (Buchs, Switzerland), Aldrich Chemical Co. (Milwaukee, WI), Riedel-deHaen AG (Seelze, Germany) and Merck Chemical Co. Nanosized TiO_2 powder was purchased from nanosabz Co. with average particle sizes of 30–50 nm. Pyromellitic dianhydride (benzen-1,2,4,5-tetracarboxylic dianhydride) (1) (from Merck Chemical CO., Germany) was purified by recrystallization from acetic anhydride follow by sublimation. DMF was dried over BaO, followed by fractional distillation. L-phenylalanine, 4,4′-thiobis(2-tert-butyl-5-methylphenol) (TTMP) were used as obtained without further purification. Coupling agent (γ-amidopropyl-triethoxyl silicane) (KH550) obtained from Merck Chemical Co.

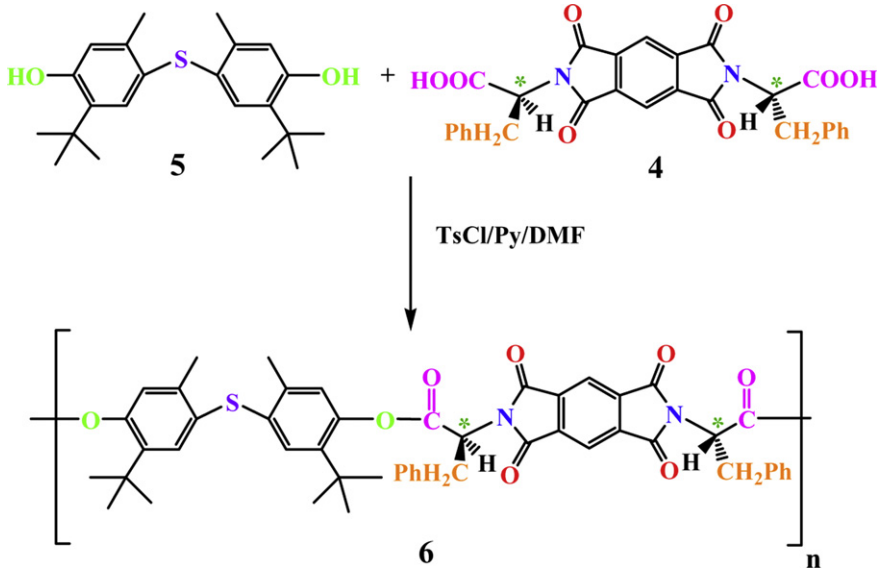

Scheme 2. Synthesis of the PEI.

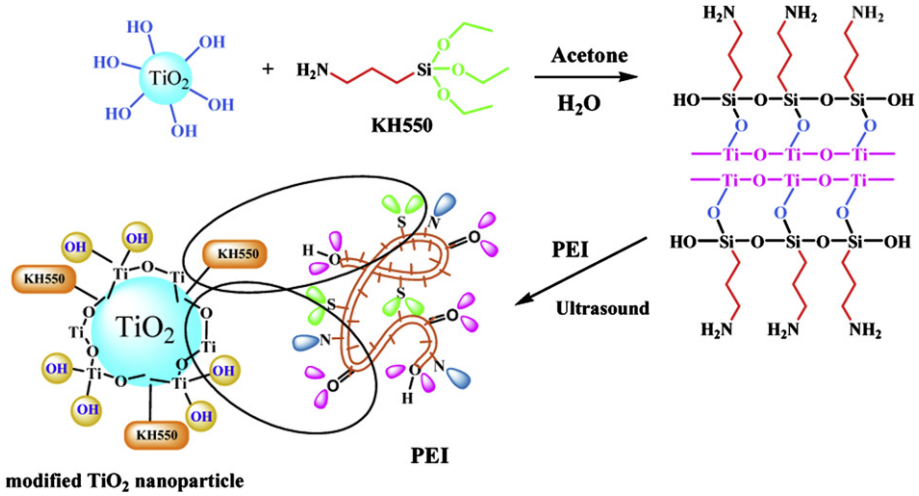

Fig. 1. Preparation of PEI/TiO_2 bionanocomposites.

2.2. Equipments

Proton nuclear magnetic resonance (^{1}H NMR, 500 MHz) spectra were carried out at a Bruker (Germany) Avance 500 instrument at room temperature (RT) in dimethylsulphoxide-d_6 (DMSO-d_6) using TMS ($Si(CH_3)_4$) as an international reference. Multiplicities of proton resonance were designated as singlet (s), doublet (d), and multiplet (m). FT-IR spectra were recorded on a spectrophotometer (Jasco-680, Japan). The spectra of solids were obtained using KBr pellets. The vibrational transition frequencies are reported in wave numbers (cm^{-1}). Band intensities are assigned as weak (w), medium (m), shoulder (sh), strong (s) and broad (br). Inherent viscosities were measured by using a Cannon–Fenske Routine Viscometer (Germany) at the concentration of 0.5 g/dL at 25 °C. Specific rotations were measured by a Jasco Polarimeter (Japan). Thermal gravimetric analysis (TGA) data for polymers were taken on a STA503 WinTA instrument in a nitrogen atmosphere at a rate of 20 °C/min. Elemental analyses were performed by Isfahan University, Isfahan, I.R. Iran. The XRD patterns of the polymer and nanocomposites were recorded using a Philips X'PERT MPD with a copper target at 40 kV and 35 mA and Cu Kα $\lambda = 1.54$ Å in the range 10–80° at the speed of 0.05°/min. Atomic force microscopy)AFM(topographic images were obtained using Digital Multimode Instruments Nanoscope III (Digital Instrument Inc.,USA) with noncontact tapping mode with a silica probe (NSC 11) and a frequency of 463 kHz. Transmission electron microscopy (TEM) analyses were performed using a Philips CM 120 operating at 100 kV. Field emission scanning electron microscopy (FE-SEM) was acquired by JSM-6700S Japan. Scanning electron microscopy (SEM) was obtained on the microscope of Cambridge Oxford (UK) 7060 with four-quadrant backscattered electron detector and with resolution 1/38 eV. The reaction was carried out on a MISONIX ultrasonic liquid processors, XL-2000 SERIES. Ultrasound was a wave of frequency 2.25×10^4 Hz and power 100 W.

2.3. Monomer synthesis

N,N′-(pyromellitoyl)-bis-L-phenylalanine diacid (4) was prepared according to our previous works [26] and is shown in Scheme 1.

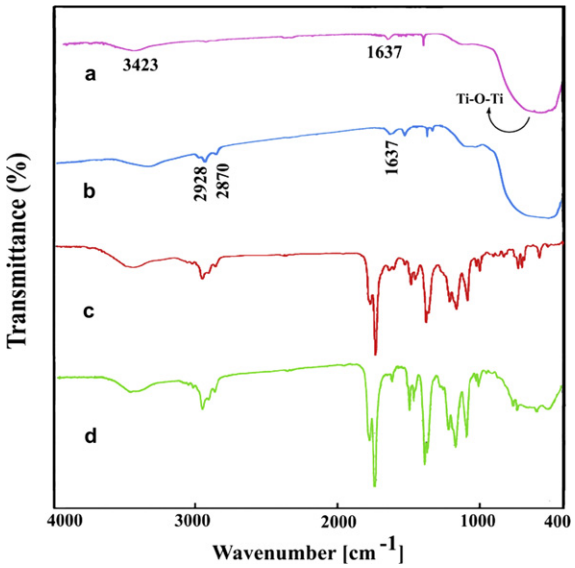

Fig. 2. FT-IR spectra of (a) pure TiO_2 nanoparticles, (b) TiO_2 nanoparticles modified by KH550 (c) pure PEI (d) PEI/TiO_2 (5 wt%).

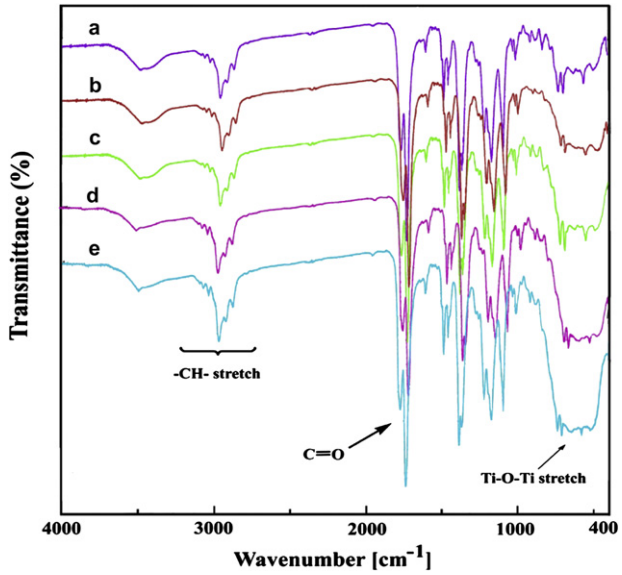

Fig. 3. FT-IR spectra of (a) PEI/TiO_2 (5 wt%), (b) PEI/TiO_2 (10 wt%), (c) PEI/TiO_2 (15 wt%), (d) PEI/TiO_2 (20 wt%), (e) PEI/TiO_2 (25 wt%).

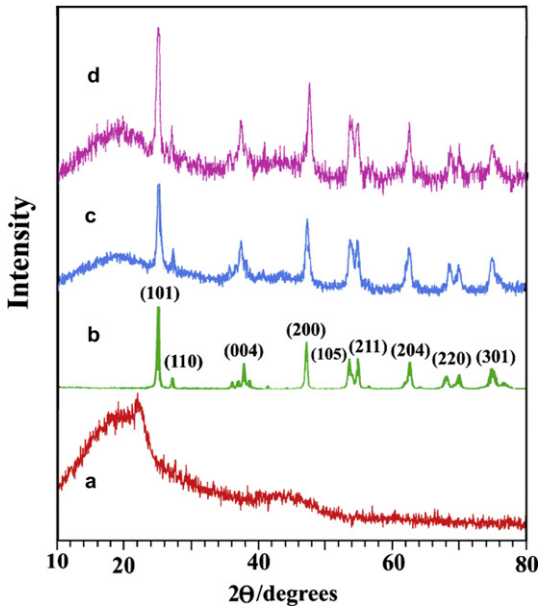

Fig. 4. XRD curves of (a) PEI (b) pure TiO_2 nanoparticles (c) PEI/TiO_2 (10 wt%), (d) PEI/TiO_2 (15 wt%).

2.4. Polymer synthesis

PEI 6 was synthesized by the direct polycondensation reaction of an equimolar mixture of diol 5 with diacid 4 in a system of TsCl/Py/DMF as condensing agent (Scheme 2). For the polymerization of optically active diacid with aromatic diol, a Vilsmeier adduct was prepared by the following procedure: a solution of Py (0.20 ml; 2.5×10^{-3} mol) with TsCl (0.18 g; 9.75×10^{-4} mol) after 30 min stirring at room temperature, was treated with DMF (0.09 ml; 1.22×10^{-3} mol) for 30 min and the mixture was added dropwise to a solution of diacid (4) (0.10 g; 1.95×10^{-4} mol) in Py (0.20 ml). The mixture was maintained at room temperature for 30 min and then TTMP (5) (0.07 g; 1.95×10^{-4} mol) was added and the whole solution was stirred at 120 °C for 6 h. Then the viscous liquid was precipitated in 30 ml of methanol to yield 0.14 g (86%) of the polymer 6. The inherent viscosity of the resulting PEI was obtained 0.17 dL/g. The amalgamation of a chiral unit into the polymer backbone was obtained by measuring the specific rotation of polymer ($[\alpha]_D^{25}$). It was obtained to be +22 (measured at a concentration of 0.5 g/dL in DMF at 25 °C).

FT-IR (KBr, cm^{-1}): 3438 (w, br), 3028 (w), 2959 (m), 2869 (w), 1765 (s), 1729 (s), 1638 (w), 1603 (w), 1525 (w), 1482 (w),1455 (w), 1380 (s), 1366 (m), 1217 (m), 1171 (m), 1093 (m), 1032 (w), 1010 (w), 728 (m). ^1H NMR (500 MHz, DMSO-d_6, δ, ppm): 0.9–1.2 (S, 18H), 2.15–2.24 (S, 6H), 3.42 (m, 2H), 3.62 (m, 2H), 5.58 (m, 2H), 6.75–7.16 (m, 14H, Ar–H), 8.26 (s, 2H), 9.66 (s, OH end group) ppm.

Elemental analysis: calcd. for ($C_{50}H_{46}N_2O_8S$): C, 71.92%; H, 5.55%; N, 3.36%; S, 3.84%. Found: C, 71.42%; H, 5.57%; N, 3.76%; S, 3.99%.

2.5. Preparation of PEI/TiO_2 bionanocomposites

The preparation of PEI/TiO_2 bionanocomposites was carried out by the following procedure: TiO_2 nanoparticles (0.3 g) was added into acetone (10 mL), and 10 wt% of silane coupling agent (KH550) was dissolved in H_2O (10 mL). Then the mixture of nanoparticles and KH550 was irradiated under ultrasonic radiation for 30 min, after that centrifuged and dried. Different amounts of modified TiO_2 nanoparticles (5, 10, 15, 20, 25 wt%) were mixed with the new PEI and the mixture was dispersed in 20 mL of absolute ethanol and then irradiated under ultrasound waves for 4 h. The resulting mixture was centrifuged. The obtained solid was dried in vacuum at 80 °C for 2 h.

3. Results and discussion

3.1. Fabrication of PEI/TiO_2 bionanocomposites

Fabrication of PEI/TiO_2 bionanocomposites was performed by an ultrasonic irradiation technique [27]. The process is depicted in Fig. 1. Under ultrasonic conditions, the coupling agent KH550 hydrolyzes to form hydroxyls and then polycondensation will occur to form Si–O–Si bonds. On the other hand hydroxyl group on the surface of TiO_2 will replace with OEt of the KH550 to link to it. Commonly, the main effects of sonication are because of cavitation or the growth and explosive disintegration of microscopic bubbles on a microsecond timescale. At the same time, ultrasonic cavitation can generate a rigorous environment of local temperature up to 5000 K and local pressure up to 500 atm [28]. Under such conditions the modified TiO_2 nanoparticles which have polar group of coupling agent and OH group on the surface of TiO_2, could be dispersed completely in polymer matrix via different interactions with the functional groups of the obtained PEI. Although the resulting PEI has lots of polar groups such as carbonyl, nitrogen and sulphur, but with respect to these functional groups they are not much difference between FT-IR spectra of resulting bionono-composites with that of pure PEI (Fig. 2) except for the Ti–O–Ti bands which proves the presence of TiO_2 in the PEI matrix. Thus, the relatively weak interaction is thought to be a hydrogen bond, and also short-ranged steric and electrical interaction between active sites of TiO_2 and different functional groups of PEI. As a result the polymer on the nanoparticle surface has a steric dispersing and stabilizing effect, which can be observed from the photographs of TEM and SEM.

3.2. Spectral data

FT-IR spectra of pure TiO_2 nanoparticles (a), TiO_2 modified by KH550 (b), pure PEI (C), PEI/TiO_2 (5 wt%) (d) are represented in Fig. 2. In pure TiO_2, OH stretching and bending bands are observed at 3423 and 1637 cm^{-1}, respectively. The broader bands at 3500 and 3422 cm^{-1} were credited to hydroxyl groups on different sites and some various interactions between hydroxyl groups on TiO_2, respectively [29]. A broad absorption peak at 500–800 cm^{-1} is assigned to the Ti–O–Ti stretching band. In the case of TiO_2 modified by KH550, The peak at 2870–2928 cm^{-1} is attributed to CH stretching band of KH550, that these stretching bands are not observed in pure TiO_2. The FT-IR spectrum of pure PEI showed the characteristic absorptions of imide and ester groups around 1765 and 1725 cm^{-1}, which are related to carbonyls stretching of imide and ester groups, respectively. The peaks at 1380 and 727 cm^{-1} show the existence of the imide heterocycle in this polymer. FT-IR spectrum of PEI/TiO_2 (5 wt%) is shown in Fig. 2(d), where the characteristic peaks of pure PEI and TiO_2 are still maintained, it may be proved that the structure of PEI was affected by the presence of TiO_2.

FT-IR spectrums of bionanocmposites with different amounts of TiO_2 (5, 10, 15, 20, 25 wt%) nanoparticles are shown in Fig. 3. From these data it is clear that with increasing the amount of nanoparticles the intensity of absorption related to Ti–O–Ti bonds was enhanced.

3.3. X-ray diffraction data

Fig. 4 shows XRD curves of PEI (a), pure TiO_2 (b), PEI/TiO_2 (10 wt %) (c) and PEI/TiO_2 (15 wt%) (d). The broad peak in XRD curve of PEI shows that the PEI in the absence of TiO_2 nanoparticles is

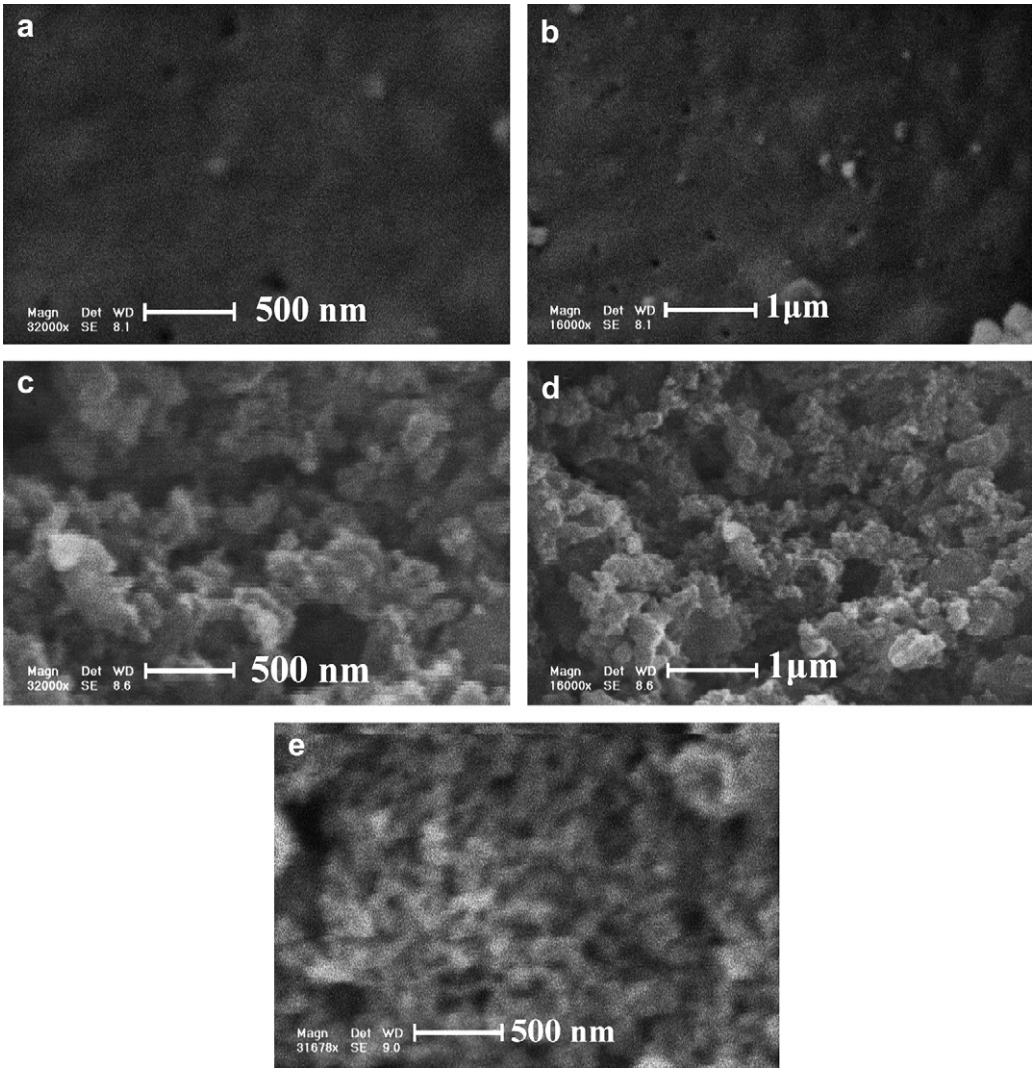

Fig. 5. SEM micrographs of (a and b) pure PEI, (c and d) PEI/TiO_2 (10 wt%), (e) PEI/TiO_2 (15 wt%).

amorphous. Presence of the non-coplanar and twisted units into the backbone of polymer decreased the intermolecular forces between the polymer chains and reduced the crystallinity of this polymer. Fig. 4(b) shows anatase and rutile phase for pure TiO_2 nano particles. The XRD patterns of PEI/TiO_2 bionanocomposites (c) and (d) show characteristic peaks of anatase and rutile of TiO_2 and PEI, respectively, indicating that the morphology of TiO_2 nanoparticles has not been disturbed during the process. The wide weak diffraction peak of PEI still exists, but its intensity decreases. The average crystalline size of nano-TiO_2, which has been determined

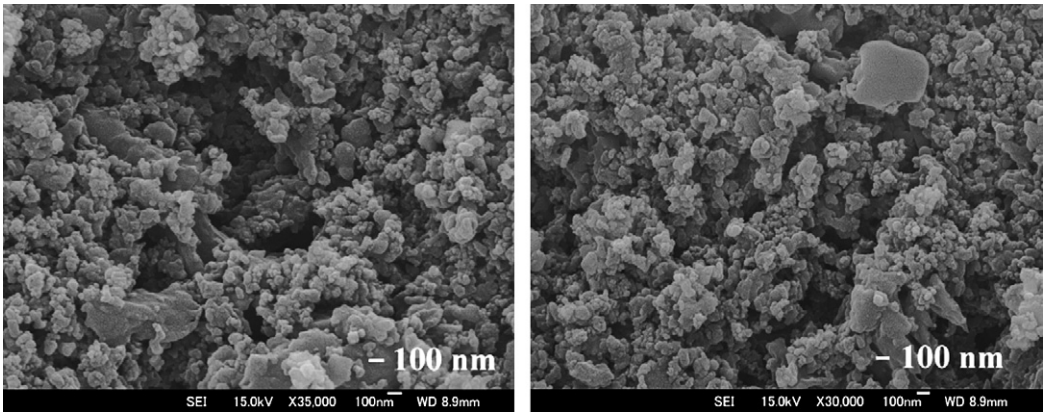

Fig. 6. FE-SEM micrographs of PEI/TiO_2 (10 wt%).

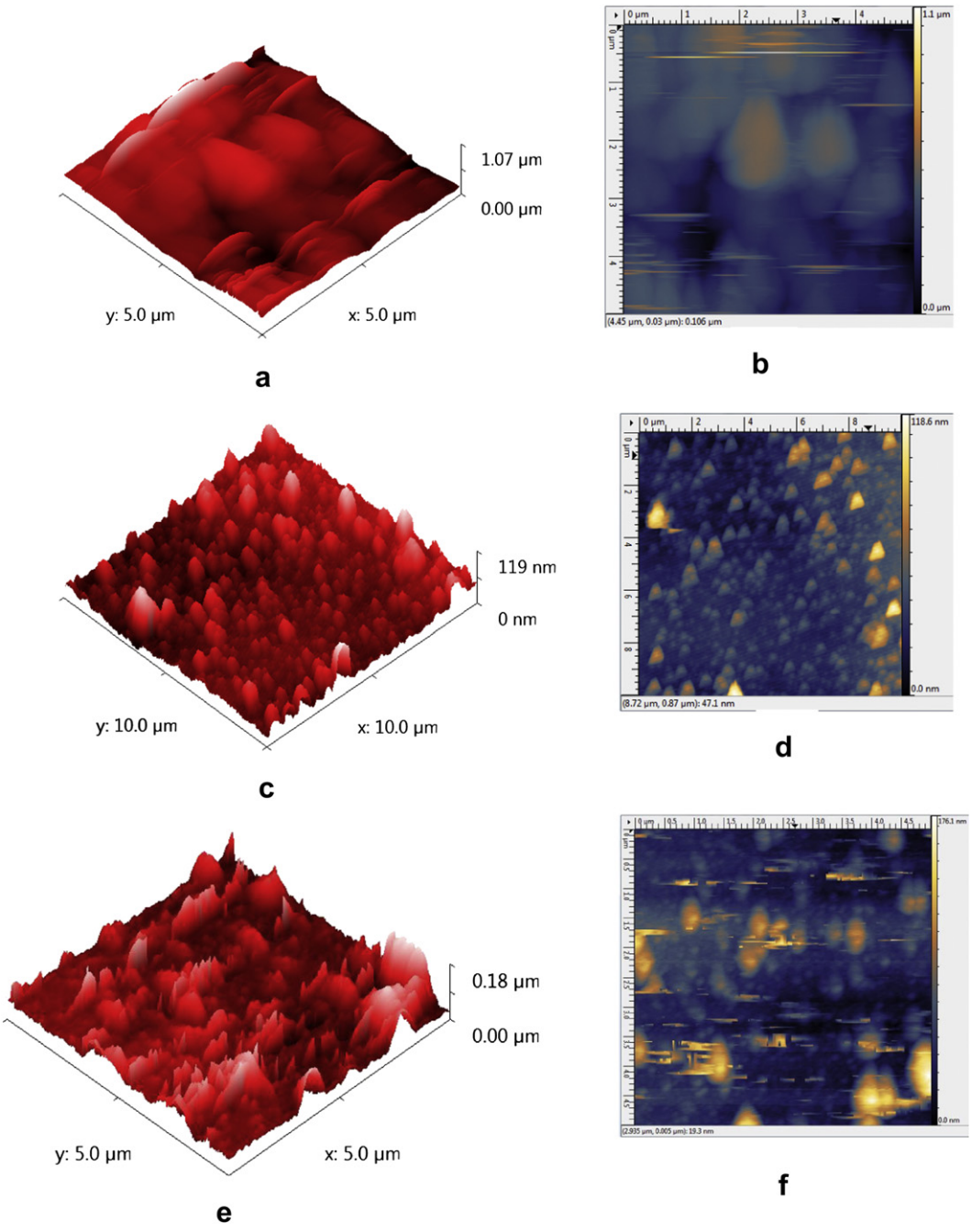

Fig. 7. The two and three dimension AFM topography images of (a and b) pure PEI, (c and d) PEI/TiO_2 (10 wt%), (e and f) PEI/TiO_2 (15 wt%).

from the half-width of the diffraction using the Debye–Scherrer equation, is approximately 15 nm. Sherrer's equation is as follows: [30]

$$D = \frac{0.9\lambda}{\beta\cos\theta}$$

Where D is the crystallite size, λ is wavelength of the radiation, θ is the Bragg's angle and β is the full width at half maximum.

3.4. Morphology

Fig. 5 shows the SEM of pure PEI (a and b), PEI/TiO_2 (10 wt%) (d and c) and PEI/TiO_2 (15 wt%) (e) nanocomposites, which indicates good compatibility and homogeneous distribution of nanoparticles in the polymer matrix. FE-SEM images of PEI/TiO_2 (10 wt%) is illustrated in Fig. 6. As can be seen, the bionanocomposite offered a homogeneous microstructure and dispersed as global beads.

Surface topography of the bionanocomposites was investigated by AFM. The three and two dimension AFM images of the pure PEI, PEI/TiO_2 (10 wt%) and PEI/TiO_2 (15 wt%) are displayed in Fig. 7. Compared with the surface morphology of pure PEI and surface morphology of PEI bionanocomposites, a number of small bulges are observed on the surface. The size of the bulge was enhanced with an increase of TiO_2 nanoparticles content in the PEI, therefore the bulges should be TiO_2 nanoparticles, indicating that some TiO_2 nanoparticles exist at PEI surface and appear in nanoscale comparing with smooth surface of pure PEI.

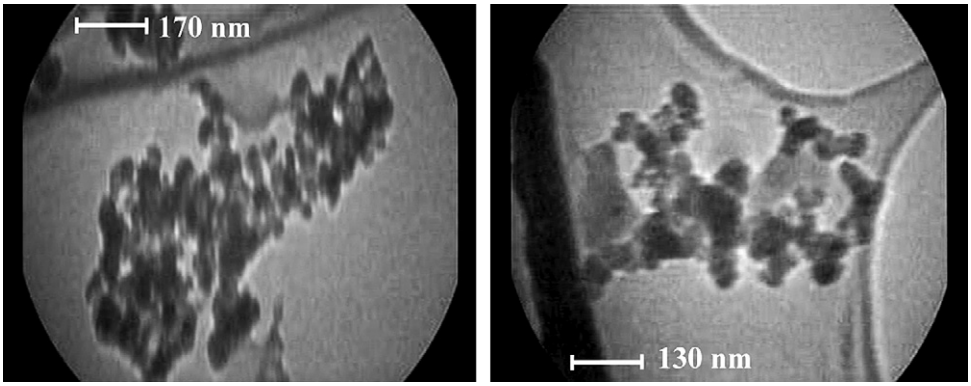

Fig. 8. TEM micrographs of PEI/TiO_2 (15 wt%).

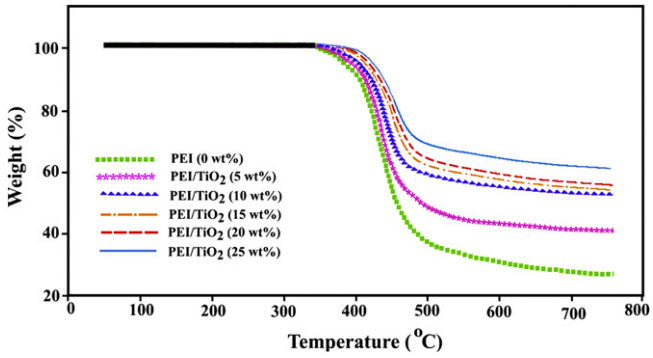

Fig. 9. TGA thermograms of PEI and PEI/TiO_2 bionanocomposites under a nitrogen atmosphere at heating rate of 20 °C/min.

Fig. 8 shows the TEM micrographs of PEI/TiO_2 (15 wt%) bionanocomposite. Some discrete TiO_2 domains and homogeneously and well-dispersed in PEI matrix are observed obviously. The nano particle sizes of TiO_2 are in the range of 30–70 nm.

4. Thermal properties

The thermal properties of the PEI and PEI/TiO_2 bionanocomposites were evaluated by TGA at a heating rate of 20 °C/min, under a nitrogen atmosphere (Fig. 9). Table 1 shows the data for the thermal degradation of the PEI and its bionanocomposites, including the temperature at which 5% (T_5) and 10% degradation occurs (T_{10}), char yield at 800 °C and also limiting oxygen index (LOI) [31].

Table 1
Thermal properties of the PEI and PEI/TiO_2 bionanocomposites.

Polymer	T_5 (°C)[a]	T_{10} (°C)[b]	Char Yield(%)[c]	LOI[d]
PEI	387	410	26	27.9
PEI/TiO_2 (5 wt%)	394	417	41	33.9
PEI/TiO_2 (10wt%)	408	423	53	38.7
PEI/TiO_2 (15 wt%)	412	425	55	39.5
PEI/TiO_2 (20 wt%)	417	429	57	40.3
PEI/TiO_2 (25 wt%)	424	433	62	42.3

[a] Temperature at which 5% weight loss was recorded by TGA at heating rate of 20 °C/min under a nitrogen atmosphere.
[b] Temperature at which 10% weight loss was recorded by TGA at heating rate of 20 °C/min under a nitrogen atmosphere.
[c] weight percentage of material left undecomposed after TGA analysis at a temperature of 800 °C under a nitrogen atmosphere.
[d] Limiting oxygen index (LOI) evaluating char yield at 800 °C.

$$LOI = 17.5 + 0.4CR$$

where CR = char yield.

From these data it is clear that the PEI had a high decomposition temperature of about 380 °C, which was further improved when TiO_2 was introduced. Incorporation of inorganic nanoparticles in polymer matrix improves its thermal stability. Increasing in the thermal stability may consequence from the high thermal stability of TiO_2 network and the physical crosslink points of the TiO_2 particles, which restricted the movement of the molecular chain of PEI. The char yield of pure PEI at 800 °C are 26%, whilst those of the bionanocomposites (PEI/TiO_2 5, 10, 15, 20, 25 wt%) at 800 °C are in the range of 41–62%, they were enhanced with an increase of TiO_2 nanoparticles content in the PEI. The high weight residue of the PEI can be arisen from the participation of thermally stable aromatic rings and imide group in its repeating unit and the rigid architecture of this polymer.

5. Conclusions

In the present study, a novel thermally stable and optically active PEI was successfully prepared by direct polycondensation method. The polymerization was carried out by the reaction of natural amino acid based diacid (4) with aromatic diol TTMP (5) using TsCl/DMF/Py as condensing agent. The prepared PEI is thermally stable and soluble in common organic solvents. Novel PEI/TiO_2 bionanocomposites were synthesized by ultrasonic method as a simple and inexpensive route to prepare the polymer/nanoparticles, using TiO_2 nanoparticles modified by KH550. The surface modification of inorganic particles by similar molecular chains to those of an organic matrix is a useful way to improve the compatibility between the organic and the inorganic phases. The modification would make the nanoparticles scatter within the matrix more homogeneously. Moreover, the molecules grafted onto the nanoparticles would interact with the matrix, thus the final mechanical properties could be greatly improved. Morphology study of resulting bionanocomposites showed well-dispersed TiO_2 nanoparticles in the polymer matrix by AFM, SEM, FE-SEM and TEM analyses. TGA studies indicated that thermal stability of the bionanocomposites has enhanced with increasing nanoparticles content. FT-IR and XRD data also confirmed that TiO_2 nanoparticles are dispersed in the PEI matrix. Since this PEI has amino acid in its polymer architecture, it could be categorized under environmentally benign polymers and could be composted with organic wastes and recycled to enrich the soil. Also, it has the potential to be used as optically active packing materials in column chromatography for the resolution of racemic mixtures. Polymers that are synthesized from naturally occurring building blocks such as amino acids are

favorable materials for pharmaceutical and biomedical purposes since their degradation products are nontoxic and can be metabolized correctly by alive tissues. Combining nanosized bioactive materials with biopolymer could produce materials with greater bioactivity and better mechanical properties. Therefore, having both natural amino acid and TiO_2 nanoparticles in these novel nanocomposites it would be suitable to name them as bionanocomposites polymers which may be anticipated to have biodegradability and biocompatibility properties.

Acknowledgements

We wish to express our gratitude to the Research Affairs Division Isfahan University of Technology (IUT), Isfahan, for partial financial support. Further financial support from National Elite Foundation (NEF), Iran Nanotechnology Initiative Council (INIC) and Center of Excellency in Sensors and Green Chemistry Research (IUT) is gratefully acknowledged. We also extend our thanks to Dr. A. Ashrafi for his valuable discussion.

References

[1] Yoshida M, Prasad PN. Chem Mater 1996;8:235–41.
[2] Zhang J, Wang BJ, Ju X, Liu T, Hu TD. Polymer 2001;42:3697–702.
[3] Zhang J, Ju X, Wang BJ, Li QS, Liu T, Hu TD. Synth Met 2001;118:181–5.
[4] Nakane K, Kurita T, Ogihara T, Ogata N. Compos B Eng 2004;35:219–22.
[5] Su SJ, Kuramoto N. Synth Met 2000;114:147–53.
[6] Coutinho CA, Gupta VK. J Colloid Interface Sci 2007;315:116–22.
[7] Rozenberg BA, Tenne R. Prog Polym Sci 2008;33:40–112.
[8] Džunuzovic E, Marinović-Cincovic M, Vuković J, Jeremić K, Nedeljković JM. Polymer Compos 2009;30:737–42.
[9] Prashantha K, Rashmi BJ, Venkatesha TV, Lee JH. Spectrochim Acta A 2006;65:340–4.
[10] Sasaki T, Beck KM, Koshizakai N. Appl Surf Sci 2002;197–198:619–23.
[11] Ohtani B, Azuma S, Nishimoto S, Kagiya T. Polym Degrad Stab 1992;35:53–60.
[12] Zan L, Fa W, Wang S. Environ Sci Technol 2006;40:1681–5.
[13] Ohtani B, Adzuma S, Miyadzo H, Nishimoto S, Kagiya T. Polym Degrad Stab 1989;23:271–8.
[14] Zan L, Wang S, Fa W, Hu Y, Tian L, Deng K. Polymer 2006;47:8155–62.
[15] Kim SH, Kwak SY, Suzuki T. Polymer 2006;47:3005–16.
[16] Ray SS. Mater Res Bull 2002;37:813–24.
[17] Price GJ, Lenz EJ, Ansell CWG. Eur Polymer J 2002;38:1531–6.
[18] Qiu XF, Zhu JJ. Chin J Inorg Chem 2003;19:766–70.
[19] Mason TJ, editor. Chemistry with ultrasound. London and New York: Society of Chemical Industry by Elsevier Applied Science; 1991. p. 1.
[20] McNamara III WB, Didenko YT, Suslick KS. Nature 1999;401:772–5.
[21] Xiang XJ, Qian JW, Yang WY. J Appl Polym Sci 2006;100:4333–7.
[22] Liaw DJ, Fan CL, Lin CC, Wang KL. J Appl Polym Sci 2004;92:2486–93.
[23] Feng L, Hu J, Liu Z, Zhao F, Liu G. Polymer 2007;48:3616–23.
[24] Vandermeulen GWM, Klok HA. Macromol Biosci 2004;4:383–98.
[25] Mallakpour SE, Hajipour AR, Faghihi K. Polym Int 2000;49:1383–8.
[26] Mallakpour SE, Hajipour AR, Habibi S. J Appl Polym Sci 2002;86:2211–6.
[27] Chen J, Zhou Y, Nan Q, Ye X, Sun Y, Zhang F, et al. Eur Polymer J 2007;43:4151–9.
[28] Chen J, Zhou YM, Nan QL, Ye XY, Sun YQ, Wang ZQ, et al. Appl Surf Sci 2008;255:2244–50.
[29] Chen J, Zhou Y, Nan Q, Sun Y, Ye X, Wang Zh. Appl Surf Sci 2007;253:9154–8.
[30] Nakayama N, Hayashi T. Polym Degrad Stab 2007;92:1255–64.
[31] Van Krevelen DW, Hoftyzer PJ. Properties of polymers. 3rdedn. Amsterdam: Elsevier; 1976.